

Theoretical approach to the fracture of two-phase glass-crystal composites

N. MIYATA, H. JINNO

Department of Industrial Chemistry, Faculty of Engineering, Kyoto University, Kyoto, Japan

This paper proposes a fracture theory for two-phase glass-crystal composites. It is hypothesized that the fracture mechanisms of such solids consist of the processes of crack nucleation and of crack propagation round the dispersed particles. At lower volume fractions of dispersed phase, macroscopic fracture will occur as a result of the growth of the micro-cracks originating in the vicinity of the pre-existing structural imperfections through a heterogeneous nucleation process; in this case, strength decreases with the proportion of the dispersed phase. At higher volume fractions where further crack propagation is prohibited by the hard crystalline particles, the process of crack propagation round the dispersed particles may be responsible for the macroscopic fracture of the composite; in this case, strength is an increasing function of the volume fraction. Expressions are formulated for mechanical strength of the glass-crystal composites, based upon the nucleation theory and Griffith's criterion. The published data on the strength of glass-alumina composites are used for the verification of the theory. The proposed theory explains well the strength behaviour of glass-alumina composites, and in particular, the dependence of the strength reduction on particle size at lower volume fractions.

1. Introduction

Numerous ceramic materials consist of a dispersed crystalline phase embedded in a glassy matrix. One can therefore regard them as composite materials of dispersion type. The properties of composite materials depend upon not only the properties of the individual phases, but also their physical and chemical interactions.

The strength of glass-crystal composites has long been studied by several investigators. Experimental data have been published for mechanical strength of such solids, including glass-alumina [1-4], glass-zirconia [1, 4, 5], glass-thoria [6] and so on. Theoretical work was done by Hasselman and Fulrath [2] to analyse the effects of particle size and volume fraction of the crystalline phase on mechanical strength of glass-crystal composites free of internal stresses. They hypothesized that hard crystalline particles dispersed within the glass matrix will limit the size of the Griffith flaws, and strengthen the composite. Based upon this criterion, they derived the expressions for mechanical strength of glass-crystal composites as below;

$$\sigma = \sigma_0(1 - \phi)^{-1/2} \quad (1)$$

for lower volume fractions or larger particle sizes at which the flaw size is smaller than the average distance between particles, and

$$\sigma = [3\gamma E \phi / \pi R(1 - \phi)]^{1/2} \quad (2)$$

for higher volume fractions or smaller particle sizes at which the average flaw size is governed by the average distance between particles. Here, σ is the fracture strength of the composite, σ_0 the fracture strength of glass matrix, R the radius of a crystalline particle, ϕ the volume fraction of dispersed particles, E and γ the Young's modulus and surface energy of the glass matrix, respectively. They interpreted their experimental results on glass-alumina composites, using their derived expressions. They obtained good agreement with their theory in the region of smaller mean distances between particles. In the region of larger mean distances, however, the dependence of the strength reduction on particle size was found. They attributed this deviation from their theory to the stress concentration due to differences in elastic properties of the two phases.

This paper is concerned with the effects of particle size and volume fraction of the crystal-

line oxide phase on mechanical strength of two-phase glass-crystal composites. A fracture theory is proposed for a model glass-crystal system, and expressions are formulated for mechanical strength of such solids, based upon the nucleation theory [7-10] and Griffith's criterion. The theory will explain well the strength reduction depending upon the particle size in the region of lower volume fractions.

2. Proposed theory

2.1. General considerations

The fracture mechanisms of glass-crystal composites are assumed to be composed of two processes: the process of crack nucleation and the process of crack propagation round the dispersed particles.

In general, when increasing tensile stress is applied to a glass-crystal composite, the micro-cracks will first originate at the weaker sites in the system through a heterogeneous nucleation process. In the glass-crystal system where hard crystalline particles are embedded in a glass matrix, the weaker sites are assumed to lie in the matrix region close to the glass-crystal interface, in which structural imperfections may be highly concentrated, and macroscopic stress concentrations may rise because of differences in elastic properties of the two phases. The micro-cracks will originate in the vicinity of the apex of the structural imperfections such as pre-existing sub-micro-cracks (Griffith flaws) which are regarded as the origins of initiating nuclei of critical size. Taking into account the stress-concentration factor, one may establish the rate of crack nucleation. In the region of larger mean distances between particles (e.g. lower volume fractions), these micro-cracks grow spontaneously in the glass matrix immediately after the crack formation and result in the macroscopic fracture of the composite. On the other hand, in the region of smaller mean distances between particles (higher volume fractions) where further crack propagation is prohibited by the crystalline particles, the micro-cracks formed by the crack-nucleation process may cease to grow further after they have grown to the size of the mean distance between particles. After some increase in the applied tensile stress, these cracks may propagate round the dispersed particles by a process involving a high surface energy in the crack, which leads to ultimate rupture of the composite.

In Fig. 1, these hypotheses are schematically illustrated. In the present work, we define

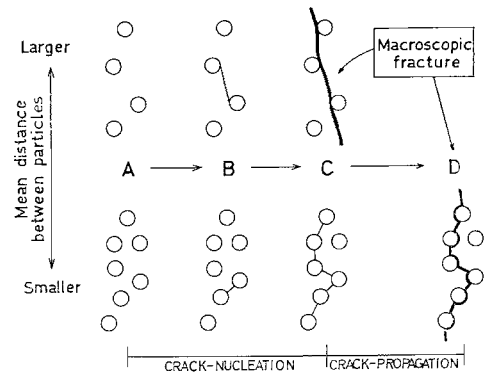


Figure 1 Proposed fracture mechanisms of glass-crystal composites.

“crack-nucleation process” as a process in which a certain number of micro-cracks nucleate individually at the matrix region between particles (change from A to C in Fig. 1). We also define “high-energy crack-propagation process” as a process in which the isolated micro-cracks formed by the crack-nucleation process, propagate round the dispersed particles (change from C to D in Fig. 1).

On the basis of the above considerations, expressions will be derived for mechanical strength of glass-crystal composites.

2.2. Macroscopic and microscopic stress concentrations

The macroscopic stress concentrations due to differences in elastic properties have been considered by Hasselman and Fulrath [3, 12]. The term, “macroscopic stress concentration” which will be used hereafter corresponds to “micro-mechanical stress concentration” according to their terminology. As being pointed out by them, Goodier's solutions [11] for the stress concentrations around a circular inclusion in a flat plate may give the best approximation to the stress condition around the dispersed particles in the specimen surface. Maximum stress occurs at the interface between matrix and circular inclusion. Under condition of a tensile load, if the elastic modulus of the inclusion is higher than that of surrounding matrix, tensile stresses greater than the applied stress occur for the radial component of the stress. When Young's modulus of the inclusion is about five times higher than that of the surrounding matrix (e.g. glass-alumina system), the maximum stress-concentration factor is about 1.4. This occurs at

two points on the perimeter of the inclusion for the uniaxial tension case, and on the whole perimeter of the inclusion for the biaxial tension case.

There are other stress concentrations than macroscopic stress concentrations mentioned above. The microscopic stress concentrations may arise in the vicinity of various structural imperfections (pre-existing sub-micro-cracks or other structural defects) which are supposedly present throughout the specimen surface or volume. These structural imperfections play an important role in the crack initiation, and they are assumed to be the origins of the crack nuclei (preferred nucleation sites). This type of stress concentration is usually characterized in terms of flaw size existing within the material (i.e. Griffith flaw).

2.3. Expressions for mechanical strength of glass-crystal composites

2.3.1. The model

The model used for this study consists of spherical crystalline particles of uniform radius, statistically embedded in a glass matrix of similar thermal expansion. The similarity of thermal expansions makes it possible to neglect macroscopic internal stresses set up during the cooling of composites.

2.3.2. Fundamental assumptions in the mathematical analyses

To simplify the problem, mathematical analyses were performed under the following conditions and assumptions. (1) Increasing tensile stress is applied with constant rate to a glass-crystal composite. (2) Young's modulus of dispersed phase is much higher than that of the glass matrix. (3) The matrix region close to the glass-crystal interface may be highly subjected to microscopic stress concentrations as well as macroscopic ones. We call this region an intermediate phase. (4) The nucleation and propagation of micro-cracks in the specimen surface should be considered, since a fracture generally initiates at the specimen surface, and high stress gradients away from the surface are imposed in a bend test usually used. (5) The micro-cracks formed by the crack nucleation grow spontaneously in the glass matrix, unless the further crack propagation is prohibited by the crystalline particles. (6) The initiation of a single crack nucleus is regarded as rate-determining in the nucleation process. This corresponds to the

change from A to B in Fig. 1. But it seems that the crack propagation round the dispersed particles begins when a certain number of nucleated micro-cracks exist in the matrix between particles (C in Fig. 1). Strictly speaking, some increase in stress is necessary for the formation of a certain number of micro-cracks, after initiation of the single crack (change from B to C in Fig. 1). It seems, however, that after the single crack formation, the fracture probability in a region containing the nucleated crack may increase considerably. In our mathematical treatment, as a first approximation, it is assumed that sufficient number of micro-cracks for the beginning of the crack propagation round the dispersed particles initiate immediately after the single crack formation. (7) Although the stress concentration should be characterized by distribution function, an average value of the stress-concentration factor will be used in this paper.

2.3.3. Crack-nucleation process

We assume that the rate of formation of crack nuclei in the glass-crystal system is given by

$$I_{\text{system}} = dn/dt = I_m + I_i + I_g .$$

Here, n is the number of nuclei and t is the time. I is the rate of formation of crack nuclei; subscripts m, i and g refer to the matrix, intermediate phase around a dispersed particle and dispersed crystalline phase, respectively. These subscripts will be used throughout this paper. In general, crystalline oxides have higher strengths than the glass matrix, so I_g may be neglected as compared with the other two terms.

Then,

$$I_{\text{system}} = I_m + I_i . \quad (3)$$

According to Fisher and others [7-10], the rate of crack nucleation in the matrix and intermediate phase are, respectively.

$$I_m = Z_m(kT/h) \exp[-(\Delta f_m^* + \Delta F_m^* - w_m)/kT] \text{ and}$$

$$I_i = Z_i(kT/h) \exp[-(\Delta f_i^* + \Delta F_i^* - w_i)/kT] ,$$

where Z is the total number of molecules which are subjected to the nucleation, k the Boltzmann's constant, h the Planck's constant, T the absolute temperature, Δf^* the free energy of activation for separating a pair of atoms as the edge of the crack moves between them, ΔF^* the maximum free energy necessary for nucleus formation and w the elastic energy contribution to Δf^* . In the

case of formation of a circular crack, ΔF_m^* and ΔF_i^* are, respectively (see Appendix I),

$$\Delta F_m^* = \pi^3 \gamma_m^3 E_m^2 / 6(1 - \nu_m^2)^2 S_m^4$$

and

$$\Delta F_i^* = \pi^3 \gamma_i^3 E_i^2 / 6(1 - \nu_i^2)^2 S_i^4,$$

where γ is the surface energy, E the Young's modulus, ν the Poisson's ratio, S the stress in the direction normal to the plane of the crack. w_m and w_i are given by

$$w_m = v_m S_m^2 / 2E_m$$

and

$$w_i = v_i S_i^2 / 2E_i,$$

respectively. Here, v is the effective volume of the vacancy created by the separation of a pair of atoms. Under condition of constant rate loading, the applied tensile stress σ in time t is rt , where r is the loading rate. We take q_m and q_i as the average combined stress-concentration factors for both phases. The value of q is assumed to be the product of microscopic and macroscopic stress-concentration factors: the one due to structural imperfections, and the other due to differences in elastic properties between matrix and dispersed phase.

S_m and S_i are then given by

$$S_m = q_m \sigma = q_m r t$$

and

$$S_i = q_i \sigma = q_i r t. \quad (4)$$

Using Equations 3 and 4, we obtain the equation for the rate of formation of crack nuclei in the system,

$$\begin{aligned} I_{\text{system}} = \frac{dn}{dt} = Z_m \frac{kT}{h} & \exp \left[-\frac{\Delta f_m^*}{kT} - \frac{\pi^3 \gamma_m^3 E_m^2}{6(1 - \nu_m^2)^2 kT q_m^4 r^4 t^4} \right. \\ & \left. + \frac{v_m q_m^2 r^2 t^2}{2E_m kT} \right] + Z_i \frac{kT}{h} \\ & \exp \left[-\frac{\Delta f_i^*}{kT} - \frac{\pi^3 \gamma_i^3 E_i^2}{6(1 - \nu_i^2)^2 kT q_i^4 r^4 t^4} \right. \\ & \left. + \frac{v_i q_i^2 r^2 t^2}{2E_i kT} \right]. \quad (5) \end{aligned}$$

As σ is given by rt , Equation 5 is written as

$$\begin{aligned} dn = Z_m \frac{kT}{rh} & \exp \left[-\frac{\Delta f_m^*}{kT} - \frac{\pi^3 \gamma_m^3 E_m^2}{6(1 - \nu_m^2)^2 kT q_m^4 \sigma^4} + \right. \\ & \left. + \frac{v_m q_m^2 \sigma^2}{2E_m kT} \right] d\sigma + Z_i \frac{kT}{rh} \\ & \exp \left[-\frac{\Delta f_i^*}{kT} - \frac{\pi^3 \gamma_i^3 E_i^2}{6(1 - \nu_i^2)^2 kT q_i^4 \sigma^4} \right. \\ & \left. + \frac{v_i q_i^2 \sigma^2}{2E_i kT} \right] d\sigma. \quad (6) \end{aligned}$$

We hypothesize that the initiation of one microcrack is the rate-determining in the crack-nucleation process. The integration of Equation 6 leads to the equation for the fracture stress, σ_1 corresponding to the nucleation of one microcrack per specimen surface. That is,

$$\begin{aligned} \int_0^1 dn = Z_m \frac{kT}{rh} \exp \left[-\frac{\Delta f_m^*}{kT} \right] \int_0^{\sigma_1} & \exp \left[-\frac{\pi^3 \gamma_m^3 E_m^2}{6(1 - \nu_m^2)^2 kT q_m^4 \sigma^4} + \frac{v_m q_m^2 \sigma^2}{2E_m kT} \right] d\sigma \\ & + Z_i \frac{kT}{rh} \exp \left[-\frac{\Delta f_i^*}{kT} \right] \int_0^{\sigma_1} \\ & \exp \left[-\frac{\pi^3 \gamma_i^3 E_i^2}{6(1 - \nu_i^2)^2 kT q_i^4 \sigma^4} + \frac{v_i q_i^2 \sigma^2}{2E_i kT} \right] d\sigma. \quad (7) \end{aligned}$$

The integrals which appear in the right-hand side of Equation 7 can not be analytically evaluated. But it is possible to obtain approximate integrations as shown in Appendix II. Hence, it follows from Equation 7 that

$$\begin{aligned} 1 = Z_m \frac{kT}{6rh} \exp \left[-\frac{\Delta f_m^*}{kT} \right] \left[\frac{\pi^3 \gamma_m^3 E_m^3}{3(1 - \nu_m^2)^2 v_m} \right]^{-B_m^{2/3}} & \left(\sigma_1 q_m \right)^{6B_m^{2/3} + 1} \\ & + Z_i \frac{kT}{6rh} \exp \left[-\frac{\Delta f_i^*}{kT} \right] \\ & \left[\frac{\pi^3 \gamma_i^3 E_i^3}{3(1 - \nu_i^2)^2 v_i} \right]^{-B_i^{2/3}} \left(\sigma_1 q_i \right)^{6B_i^{2/3} + 1} \quad (8) \end{aligned}$$

where

$$B_m = (v_m / 2E_m kT) [\pi^3 \gamma_m^3 E_m^2 / 6(1 - \nu_m^2)^2 kT]^{1/2}$$

and

$$B_i = (v_i / 2E_i kT) [\pi^3 \gamma_i^3 E_i^2 / 6(1 - \nu_i^2)^2 kT]^{1/2}.$$

We consider the case where the physical properties of the intermediate phase are not very different from those of the matrix. If $\Delta f_i^* \simeq \Delta f_m^*$, $\gamma_i \simeq \gamma_m$, $\nu_i \simeq \nu_m$, $E_i \simeq E_m$ and $v_i \simeq v_m$ are valid, Equation 8 becomes

$$\begin{aligned} (Z_m q_m^{6B_m^{2/3} + 1} + Z_i q_i^{6B_m^{2/3} + 1}) \frac{kT}{6rh} \exp \left[-\frac{\Delta f_m^*}{kT} \right] & \left[\frac{\pi^3 \gamma_m^3 E_m^3}{3(1 - \nu_m^2)^2 v_m} \right]^{-B_m^{2/3}} \sigma_1^{6B_m^{2/3} + 1} = 1. \quad (9) \end{aligned}$$

Solving Equation 9 for σ_1 and writing α to replace $6B_m^{2/3}$ for convenience, we obtain

$$\sigma_1 = \left[\frac{\pi^3 \gamma_m^3 E_m^3}{3(1 - \nu_m^3)^2 v_m} \right]^{\alpha/6(\alpha+1)} \left[\frac{(6rh/kT) \exp(\Delta f_m^*/kT)}{Z_m q_m^{\alpha+1} + Z_i q_i^{\alpha+1}} \right]^{1/(\alpha+1)}, \quad (10)$$

where

$$\alpha = (\pi \gamma_m/kT)[9v_m^2/(1 - \nu_m^2)^2]^{1/3}. \quad (11)$$

The value of σ_1 may be calculated from Equation 10 if all the physical constants are known. It should be noted that

$$\left[\frac{\pi^3 \gamma_m^3 E_m^3}{3(1 - \nu_m^2)^2 v_m} \right]^{1/6} = \left[\frac{\pi \gamma_m E_m}{3^{1/3}(1 - \nu_m^2)^{2/3} v_m^{1/3}} \right]^{1/2}$$

in Equation 10 is approximately equal to the expression for theoretical strength of glass, derived from the Griffith-Orowan's criterion. In fact, it is the second factor in Equation 10 that gives the effects of loading rate, temperature, stress concentrations, and total number of molecules subjected to crack nucleation.

We denote the fracture stress at $\phi = 0$ by σ_0 , which corresponds to the fracture strength of the glass matrix. If $Z_m = A \Delta_m \zeta_m$ at $\phi = 0$,

$$\sigma_0 = \left[\frac{\pi^3 \gamma_m^3 E_m^3}{3(1 - \nu_m^2)^2 v_m} \right]^{\alpha/6(\alpha+1)} \left[\frac{(6rh/kT) \exp(\Delta f_m^*/kT)}{A \Delta_m \zeta_m q_m^{\alpha+1}} \right]^{1/(\alpha+1)} \quad (12)$$

We assume an intermediate phase exists as a spherical shell with thickness δ around a particle with radius R . Let A be the surface area of the specimen, ϕ the volume fraction of the dispersed phase, Δ the number of preferred nucleation sites per unit area and ζ the number of molecules which are concentrated in the neighbourhood of the apex of each nucleation site. From the geometrical considerations, the total number of molecules subjected to the nucleation per specimen surface are

$$Z_m = [1 - (1 + \delta/R)^3 \phi] A \Delta_m \zeta_m$$

and

$$Z_i = [(1 + \delta/R)^3 - 1] \phi A \Delta_i \zeta_i, \quad (13)$$

respectively. Substitution of Equations 13 into Equation 5 leads to the rate of crack nucleation per specimen surface. Substituting Equations 13 into Equation 10 and combining Equations 10 and 12, one obtains

$$\frac{\sigma_1}{\sigma_0} = \left\{ 1 - \left(1 + \frac{\delta}{R} \right)^3 \phi + \left[\left(1 + \frac{\delta}{R} \right)^3 - 1 \right] \phi \frac{\Delta_i \zeta_i}{\Delta_m \zeta_m} \left(\frac{q_i}{q_m} \right)^{\alpha+1} \right\}^{-1/(\alpha+1)}. \quad (14)$$

It may be considered that $q_i/q_m > 1$ and $\Delta_i \zeta_i/\Delta_m \zeta_m > 1$. Since the value of α calculated from Equation 11 is a large number (see Section 3.1), $(1 + \delta/R)^3 \phi$ may be neglected in comparison with other terms. Moreover, the thickness of the intermediate phase is assumed to be small in comparison with a particle radius, i.e., $\delta/R \ll 1$, as far as the chemical reaction between phases are not so remarkable. Equation 14 is then simplified as

$$\frac{\sigma_1}{\sigma_0} = \left[1 + \frac{3\delta}{R} \phi \frac{\Delta_i \zeta_i}{\Delta_m \zeta_m} \left(\frac{q_i}{q_m} \right)^{\alpha+1} \right]^{-1/(\alpha+1)}. \quad (15)$$

2.3.4. High energy crack propagation process

If the average distance between particles is sufficiently larger, the micro-cracks formed by the crack-nucleation process may grow further and result in macroscopic fracture. On the other hand, when the average distance is smaller, the nucleated micro-cracks may cease to grow further after they have grown to the size of the average distance between particles, since the hard crystalline particles are assumed to prohibit the further crack propagation. In this case, the macroscopic fracture will occur through the high energy crack propagation process.

According to Griffith's criterion, the required stress for propagation of a narrow crack of length $2c$ is given by $(2\gamma_p E_m/\pi c)^{1/2}$. Here, γ_p is the effective surface energy containing contributions such as subsidiary cracking near the glass-crystal interface. So, γ_p is expected to be larger than γ_m .

We denote the macroscopic stress-concentration factor at the glass-crystal interface by Q ; this is due to differences in elastic properties between matrix and dispersed phase. In the high-energy crack-propagation process the condition for the spreading of the micro-cracks round the dispersed particles can be expressed as

$$Q \sigma_2 = (2\gamma_p E_m/\pi c)^{1/2} \quad (16)$$

where σ_2 is the applied stress. The average length of the micro-cracks formed in the crack-nucleation process is equal to the mean free path between particles, which is given by Fullman [13] as $4R(1 - \phi)/3\phi$. Then,

$$c = 2R(1 - \phi)/3\phi. \quad (17)$$

Substituting Equation 17 into Equation 16, we arrive at the expression for the fracture stress σ_2 in the high-energy crack-propagation process.

$$\sigma_2 = (1/Q)[3\gamma_p E_m \phi/\pi R(1 - \phi)]^{1/2}. \quad (18)$$

Equation 18 is formally the same as Equation 2.

3. Discussion of the theory and comparison with published work

3.1. Estimation of α

The uncertainty in the choice of values for v_m and γ_m which appear in Equation 11 makes it impossible to evaluate a value of α with accuracy. Nevertheless, we may obtain an order of magnitude for α from the following reasonable considerations.

We assume that v_m is the change in volume of one Si-O bond from the unfractured state to the fractured state and is approximately equal to a half of the volume occupied by the sphere with diameter of the bond distance. That is, since the Si-O bond distance is 1.62\AA , v_m may be estimated at about $1.11 \times 10^{-24} \text{ cm}^3$. The most important and difficult problem is the choice of the γ_m value. The surface energy has long been a subject of controversy. The published values of the fracture surface energy range from 1000 to 5000 ergs/cm², depending upon the various glass compositions and atmospheric conditions [14].

The linear relationship, $\alpha = 1.74 \times 10^{-2} \gamma_m$ may be obtained from Equation 11, if we take numerical values: $T = 300 \text{ K}$, $\nu_m = 0.20$, $k = 1.38 \times 10^{-16} \text{ ergs/K}$, $v_m = 1.11 \times 10^{-24} \text{ cm}^3$. The α value is found to be about 10 to 70 for the range of γ_m value from 600 to 4000 ergs/cm².

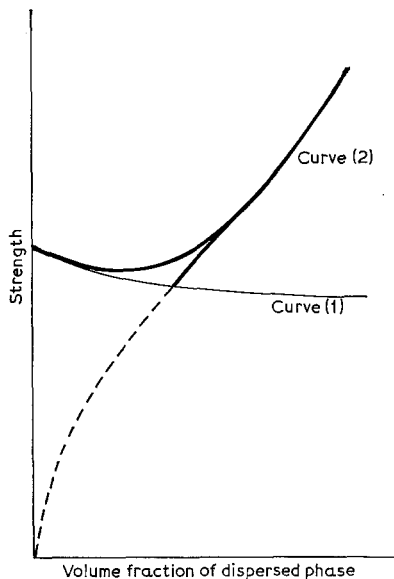


Figure 2 Schematic representation of the strength of glass-crystal composites. Curves (1) and (2) correspond to the crack-nucleation and crack-propagation process, respectively.

3.2. Theoretical strength-volume fraction curve

Equations 15 and 18 can be schematically illustrated in Fig. 2, as a function of volume fraction of dispersed crystalline phase, corresponding to each of the fracture mechanisms: curve (1) from Equation 15 and curve (2) from Equation 18. In the region of lower volume fractions, the fracture strength decreases monotonically with volume fractions. In the region of higher volume fractions, however, prohibition of crack propagation occurs, and fracture strength increases with increasing volume fractions. Curves (1) and (2) intersect in a certain volume fraction, depending upon the grain size. The measured strength-volume fraction curve will, therefore, have a minimum near the point of intersection.

3.2.1. Effect of particle size

According to Equations 15 and 18, the effect of grain size on the strength is much more important in Equation 18 than in Equation 15, since the α value is larger than about 10 as shown in Section 3.1. So, the minimum will shift to lower volume fractions with smaller particle sizes, and the strength reduction is less with finer particles.

3.2.2. Effect of macroscopic stress concentrations

As indicated in Section 2.2, differences in elastic properties between matrix and dispersed phase lead to macroscopic stress concentrations around a dispersed particle, and the maximum stress concentrations occur on the perimeter of the inclusion. The combined stress-concentration factor in the intermediate phase, q_i contains Q , the macroscopic stress-concentration factor at the glass-crystal interface. That is, $q_i/q_m \geq Q$. Under the same condition of microscopic stress concentrations, q_i/q_m is proportional to Q . Fig. 3 shows the effect of macroscopic stress concentrations. It is seen that the larger Q results in the more precipitous decrease in strength at the volume fraction closer to zero.

3.3. Comparison of the theory with published work

Hasselmann and Fulrath [2, 3] carried out systematic measurements on the strength of glass-alumina composites free of internal stresses. They measured cross-bending strengths on a sodium borosilicate glass containing varying volume fractions of spheroidized alumina over a

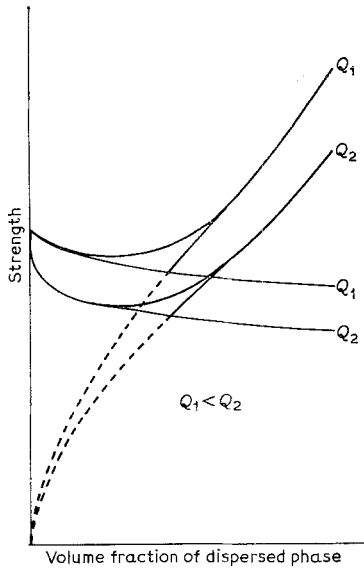


Figure 3 Effect of macroscopic stress concentrations on the strength of glass-crystal composites.

wide range of particle sizes. Here, we will assess the conformity of our theory with their experimental results a part of which are shown in Fig. 4.

Let us evaluate an order of magnitude of the exponent α from their data. Assuming that $q_i/q_m > 1.4$ (see Section 2.2), $\Delta_i \zeta_i/\Delta_m \zeta_m > 1$, and δ is an order of micron or less, we find,

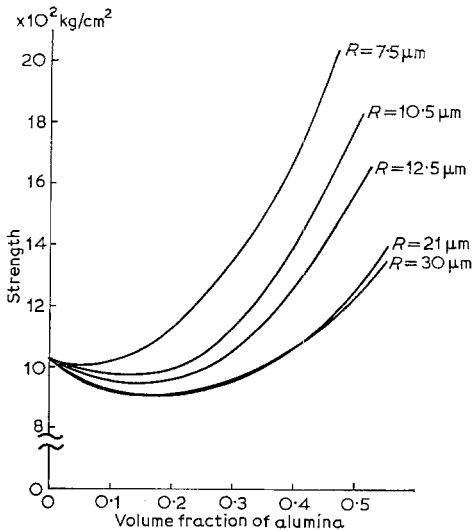


Figure 4 Cross-bending strength of glass-alumina composites as a function of volume fraction of alumina (after Hasselman and Fulrath [2, 3]).

unless ϕ is extremely close to zero, the second term in the bracket of Equation 15 is much larger than unity, since the value of α estimated from Equation 11 is a large number. So the interpretation of the experimental results in the region of lower volume fractions where strength is reduced with increasing ϕ may be carried out by the following equation,

$$\sigma_1 = \sigma_0 \left(\frac{1}{3\delta} \frac{R \Delta_m \zeta_m}{\Delta_i \zeta_i} \right)^{1/\alpha} \left(\frac{q_m}{q_i} \right).$$

When σ_1 is plotted against ϕ on logarithmic scale, linear relation should be obtained and its slope gives the value of $-1/\alpha$. Fig. 5 shows the result of the logarithmic plot. The measured values for $R = 30$ and $25.5 \mu\text{m}$ were used, because the data in the region of lower volume fractions are available and because those which are on the far left of the minimum in these curves are assumed to coincide with the curves due to crack-nucleation process. From the slope, α is estimated at the order of 14 to 18. This α value corresponds to about 1000 ergs/cm^2 for γ_m (see Section 3.1), which is the same order as the fracture surface energy of glass reported in the literature [14].

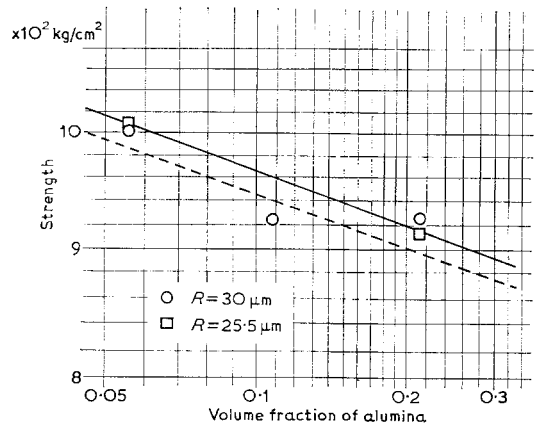


Figure 5 Logarithmic plot of the strength of glass-alumina composites at lower volume fractions (Data from Hasselman and Fulrath [2, 3]).

The region of higher volume fractions, situated on the far right of each minima in Fig. 4 corresponds to the region where Hasselman and Fulrath obtained good conformity of Equation 2 with experimental results. In the same way, we can best fit Equation 18 to the data in this region. The value of the effective surface energy

γ_p calculated by fitting the theory to the data, is about 7800 and 4000 ergs/cm², if Q is taken as 1.4 and 1.0, respectively. $Q = 1.4$ corresponds to the maximum stress-concentration factor in glass-alumina system. Under uniaxial stress conditions, however, the maximum stress concentration due to differences in elastic properties acts at the two points only on the perimeter of a dispersed particle. Therefore $Q = 1.4$ may be overestimated. In any case, the value of γ_p calculated is several times higher than γ_m obtained from the crack-nucleation curve. This difference may be explained by the assumption that γ_p contains a relatively large amount of work required for subsidiary cracking that is necessary for further crack-propagation round the dispersed particles. But this assumption contains some ambiguity, and further examination should be undertaken.

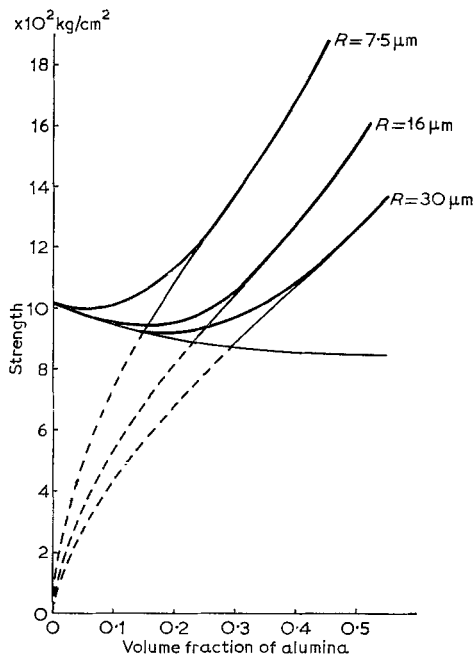


Figure 6 Comparison of the theory with the experimental data of Hasselman and Fulrath [2, 3].

Consequently the experimental results in Fig. 4 can be interpreted as Fig. 6. The data for $R = 7.5, 16$ and $30 \mu\text{m}$ were plotted. Since α is about 18, the curves due to crack-nucleation process almost overlap in the range of considered particle sizes. Then, to avoid the confusion in the figure, only one curve for $R = 30 \mu\text{m}$ is drawn

as the representative curve for crack-nucleation process. As seen from Fig. 6, it may be considered that the observed strength-volume fraction curve consists of two curves: the one due to crack-nucleation process and the other due to crack-propagation process.

Hasselman and Fulrath have also measured the biaxial strength of the same glass containing alumina spheres with radius $20 \mu\text{m}$ [3, 12]. They found that the results for biaxial tensile strength, in contrast to the uniaxial strength results, showed a precipitous decline in strength on addition of the alumina phase. This difference in strength behaviour under the two stress conditions can be explained on the basis of the discussion in Section 3.2.2 (Fig. 3). Under biaxial stress conditions the maximum stress acts over the whole perimeter of the dispersed particle. In this case, the average value of Q may be estimated at about 1.4. On the contrary, under uniaxial stress conditions, the average value of Q may be much smaller than the maximum stress-concentration factor, 1.4, since the maximum stress acts at the two points only on the perimeter.

Equation 1 proposed by Hasselman and Fulrath gives a monotonical increasing function of ϕ , and does not explain the strength behaviour at lower volume fractions. They attributed this discrepancy to stress concentration due to differences in elastic properties of the two phases and interpreted qualitatively the particle size dependence of strength reduction in terms of the volume of material subjected to stress concentration [3, 12]. Their attribution is reasonable in the sense that the macroscopic stress concentrations due to differences in elastic properties of the two phases have a considerable effect on fracture behaviour of the composite. But it seems that their interpretation is not fully sufficient for explaining the strength reduction depending upon particle size. Our theory containing the formulated expression based upon the nucleation theory, however, may lead to quantitative understanding of this strength behaviour at lower volume fractions.

4. Summary

A theoretical approach was made to the mechanical strength of two-phase glass-crystal composites. Expressions were formulated for mechanical strength of such solids, based upon nucleation theory and Griffith's criterion. Comparison of our theory with published data

on the strength of glass-alumina composites may support our hypothesis that the fracture mechanisms are composed of the processes of crack nucleation and of crack propagation round the dispersed particles. The proposed theory can explain well the characteristic strength reduction accompanied with particle size dependence at lower volume fractions of dispersed phase.

The present study is only applicable to the strength behaviour of glass-crystal composites free of internal stresses due to differences in thermal expansion coefficients of the two phases. Naturally, the effect of internal stresses on mechanical strength of the composites is very important, and further study is required.

Appendix I

The net work or free energy associated with the reversible formation of a circular crack of radius ρ may be written as

$$\Delta F = 2\pi \rho^2 \gamma - 8(1 - \nu^2) \rho^3 S^2/3E.$$

Here, $2\pi \rho^2 \gamma$ is the work required for the reversible formation of the two surfaces of a circular crack, and $-8(1 - \nu^2) \rho^3 S^2/3E$ is the decrease in the strain energy in the neighbourhood of the crack, which has been shown by Sack [15].

The curve of ΔF versus ρ has a maximum

$$\Delta F^* = \pi^3 \gamma^3 E^2/6(1 - \nu^2)^2 S^4$$

for cracks with radius

$$\rho^* = \pi \gamma E/2(1 - \nu^2) S^2.$$

Appendix II

$$\int_0^{\sigma_1} \exp \left[-\frac{\pi^3 \gamma^3 E^2}{6(1 - \nu^2)^2 kT q^4 \sigma^4} + \frac{v q^2 \sigma^2}{2E kT} \right] d\sigma \dots (A1)$$

in Equation 7 is analytically impossible. But we can obtain roughly approximated integration in the following manner.

The integral can be simplified by replacing the variable σ with

$$x = \sigma q / [\pi^3 \gamma^3 E^2/6(1 - \nu^2)^2 kT]^{1/4}$$

and by introducing the abbreviation

$$B = (v/2E kT) [\pi^3 \gamma^3 E^2/6(1 - \nu^2)^2 kT]^{1/2}$$

Then, the integral A1 can be written as

$$\left[\frac{\pi^3 \gamma^3 E^2}{6(1 - \nu^2)^2 kT} \right]^{1/4} \frac{1}{q} \int_0^{x_1} \exp \left[-\frac{1}{x^4} + Bx^2 \right] dx, \dots (A2)$$

where

$$x_1 = \sigma_1 q / [\pi^3 \gamma^3 E^2/6(1 - \nu^2)^2 kT]^{1/4}.$$

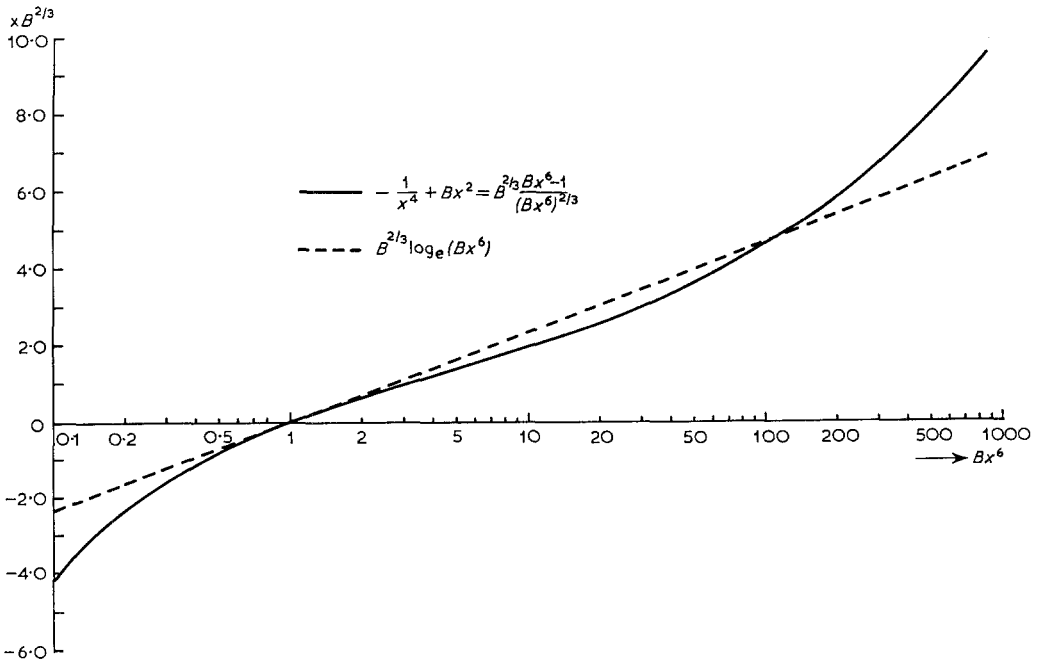


Figure A1 The terms $(-1/x^4 + Bx^2)$ and $B^{2/3} \log_e(Bx^6)$ as a function of Bx^6 .

The term $(-1/x^4 + Bx^2)$ is roughly approximated by $B^{2/3} \log_e(Bx^6)$ in the relatively wide range of x^6 . For comparison, the calculated values of these two terms are represented as a function of Bx^6 in Fig. A1. From the figure, it is seen that $B^{2/3} \log_e(Bx^6)$ may be used instead of $(-1/x^4 + Bx^2)$ in the range of $0.4 < Bx^6 < 100$ which covers the stress range where crack nucleation may occur.

Then, the substitution of $B^{2/3} \log_e(Bx^6)$ for $(-1/x^4 + Bx^2)$ leads to

$$\exp\left[-\frac{1}{x^4} + Bx^2\right] \simeq (Bx^6)^{B^{2/3}}.$$

The integral in the expression A2 becomes

$$\int_0^{x_1} (Bx^6)^{B^{2/3}} dx = \frac{B^{B^{2/3}} x_1^{6B^{2/3}+1}}{6B^{2/3} + 1}. \quad (A3)$$

The calculated value for $6B^{2/3}$ from the physical constants is much larger than unity, so we can approximately evaluate the integral A1.

$$\begin{aligned} & \int_0^{\sigma_1} \exp\left[-\frac{\pi^3 \gamma^3 E^2}{6(1-\nu^2)^2 kT q^4 \sigma^4} + \frac{\nu q^2 \sigma^2}{2E kT}\right] d\sigma \\ & \simeq \left[\frac{\pi^3 \gamma^3 E^2}{6(1-\nu^2)^2 kT}\right]^{1/4} \cdot \frac{1}{q} \cdot \frac{B^{B^{2/3}} x_1^{6B^{2/3}+1}}{6B^{2/3} + 1} \\ & \simeq \frac{1}{6} \left[\frac{\pi^3 \gamma^3 E^3}{3(1-\nu^2)^2 \nu}\right]^{-B^{2/3}} \left(\sigma_1 q\right)^{6B^{2/3}+1}. \end{aligned}$$

References

1. D. B. BINNS, "Science of Ceramics", Vol. 1 edited by G. H. Stewart (Academic Press, London, 1962) p. 315.
2. D. P. H. HASSELMAN and R. M. FULRATH, *J. Amer. Ceram. Soc.* **49** (1966) 68.
3. *Idem*, "Ceramic Microstructure", edited by R. M. Fulrath and J. A. Pask (John Wiley & Sons, New York, 1968) p. 343.
4. W. J. FREY and J. D. MACKENZIE, *J. Mater. Sci.* **2** (1967) 124.
5. R. R. TUMMALA and A. L. FRIEDBERG, *J. Amer. Ceram. Soc.* **52** (1969) 228.
6. R. W. DAVIDGE and T. J. GREEN, *J. Mater. Sci.* **3** (1968) 629.
7. J. C. FISHER, *J. Appl. Phys.* **19** (1948) 1062.
8. T. YOKOBORI, *J. Chem. Phys.* **22** (1954) 951.
9. *Idem*, *J. Phys. Soc. Japan*, **10** (1955) 368.
10. D. PREVORSEK and W. J. LYONS, *J. Appl. Phys.* **35** (1964) 3152.
11. J. N. GOODIER, *J. Appl. Mech.* **1** (1933) 39.
12. D. P. H. HASSELMAN and R. M. FULRATH, *J. Amer. Ceram. Soc.* **50** (1967) 399.
13. R. L. FULLMAN, *Trans. AIME* **197** (1953) 447.
14. S. M. WIEDERHORN, *J. Amer. Ceram. Soc.* **52** (1969) 99.
15. R. A. SACK, *Proc. Phys. Soc. (London)* **58** (1946) 729.

Received 25 October 1971 and accepted 15 February 1972